

Selection of optimal external filter for colorimetric camera

Michael J. Vrhel, Artifex Software, Novato, CA
 H. Joel Trussell, North Carolina State University, Raleigh, NC

Abstract

A database of realizable filters is created and searched to obtain the best filter that, when placed in front of an existing camera, results in improved colorimetric capabilities for the system. The image data with the external filter is combined with image data without the filter to provide a six-band system. The colorimetric accuracy of the system is quantified using simulations that include a realistic signal-dependent noise model. Using a training data set, we selected the optimal filter based on four criteria: Vora Value, Figure of Merit, training average ΔE , and training maximum ΔE . Each selected filter was used on testing data. The filters chosen using the training ΔE criteria consistently outperformed the theoretical criteria.

Introduction

The colorimetric accuracy of a digital color camera is limited by the spectral sensitivity of the optical system and the presence of noise. Both of these limitations must be considered when designing a new system or when determining how best to augment an existing device. If color filters are used in a design, it is helpful to impose constraints on the filters to ensure they can be readily manufactured.

Studies of camera noise have shown that the dominant noise source is caused by the photon counting process, which can be modeled with a Poisson probability density function [1]. For a Poisson process, the mean of the process equals the variance, which implies that the noise in the system will be signal-dependent in nature.

The spectral sensitivity of the system is generally not a linear transformation of the CIEXYZ color matching functions. This mismatch implies that colors can look the same to the human visual system but be reported as different values by the camera. Likewise, two colors that look different to the human visual system can be recorded as the same value by the camera.

There has recently been work on the problem of finding an optimal filter to place in front of a camera, resulting in an overall system that is “closer” to being within a linear transformation of the CIEXYZ color matching functions (*i.e.*, closer to satisfying the Luther condition [2]). Making use of the Vora Value [3], Finlayson and Zhu looked at finding an optimal filter [4, 5, 6, 7]. Vrhel looked at finding an optimal filter that maximized Sharma’s Figure of Merit (FOM) in the presence of signal independent noise [8]. None of these approaches considered realizability of the filters, although they did impose smoothness constraints on the solution. Realizability was used in [9], but that work involved the complete design of the system spectral response rather than altering an existing system.

Here we look at a slightly different problem, which is one where we consider that we have two images from our camera: one

obtained with a filter in front of the camera, and another without the filter, as illustrated in Figure 1. This approach effectively provides six bands of information to use. We also consider filters from a database of known available filters and make use of a realistic signal-dependent noise model in simulations. Using readily available filters makes it possible to easily move forward to the next step of capturing real image data.



Figure 1. Image captured without filter and with filter

Mathematical notation

If we assume we can mathematically sample the visible spectrum at a sufficient number of wavelengths, n , to allow an accurate representation of the spectral information [10], we can model the camera color imaging system using a vector notation. The imaging model is given by

$$\mathbf{c}_i = \mathbf{H}^T \mathbf{L} \mathbf{r}_i + \mathbf{n}_i, \quad (1)$$

where the columns of the $n \times m$ matrix \mathbf{H} define the m spectral separation channels for the camera,¹ the $n \times n$ diagonal matrix \mathbf{L} represents the illuminant under which the scene is recorded, the n -element vector \mathbf{r}_i represents the reflectance spectrum at pixel location i , the m -element vector \mathbf{n}_i represents the additive noise at location i , and \mathbf{c}_i is the m -element vector obtained at the camera pixel index location i . Note that we have used a single index i for the location for simplification.

Placing a filter with transmittance \mathbf{f} in front of the system and merging the resulting values with the unfiltered values is modeled as

$$\mathbf{d}_i = [\mathbf{H} \mathbf{H} \mathbf{F}]^T \mathbf{L} \mathbf{r}_i + \mathbf{n}_i = \mathbf{M}^T \mathbf{L} \mathbf{r}_i + \mathbf{n}_i, \quad (2)$$

where \mathbf{d}_i is the $2m$ -element vector obtained for pixel location i , $\mathbf{F} = \text{diag}(\mathbf{f})$ is a diagonal matrix whose diagonal elements are the filter transmittance values at the sampled wavelengths, \mathbf{n}_i is the noise for the filtered and unfiltered scene, and $\mathbf{M}^T = [\mathbf{H} \mathbf{H} \mathbf{F}]^T$.

¹In most cases $m = 3$.

Ideally, the complete system response would be within a linear transformation of the CIEXYZ color matching functions. In general, it is difficult to achieve this goal. Short of this goal, given the recorded value \mathbf{d}_i or \mathbf{c}_i with our camera, we wish to obtain an estimate of the CIEXYZ value of the spectrum \mathbf{Lr}_i , which is mathematically expressed as

$$\mathbf{t}_i = \mathbf{A}^T \mathbf{Lr}_i, \quad (3)$$

where the columns of the matrix \mathbf{A} are the sampled CIEXYZ color matching functions.

There are a number of ways to obtain such an estimate. One common approach is to use a linear estimator and, in particular, the linear minimum mean square error (LMMSE) estimator, since we can readily compute this estimator analytically. Working from Equation 2, for the LMMSE estimator, the matrix \mathbf{B}_{lmmse} and vector \mathbf{b}_{lmmse} are the solution to the optimization problem

$$(\mathbf{B}_{lmmse}, \mathbf{b}_{lmmse}) = \arg \min_{\mathbf{B}, \mathbf{b}} E \left\{ \|\mathbf{B}\mathbf{d} + \mathbf{b} - \mathbf{t}\|^2 \right\}, \quad (4)$$

where $E\{\cdot\}$ denotes the expectation operator. The estimated CIEXYZ tristimulus value is given by

$$\hat{\mathbf{t}}_i = \mathbf{B}_{lmmse} \mathbf{d}_i + \mathbf{b}_{lmmse}. \quad (5)$$

The solution to Equation 4 is given by

$$\mathbf{B}_{lmmse} = \mathbf{A}^T \mathbf{L} \mathbf{K}_r \mathbf{L} \mathbf{M} (\mathbf{M}^T \mathbf{L} \mathbf{K}_r \mathbf{L} \mathbf{M} + \mathbf{K}_n)^{-1} \quad (6)$$

$$\mathbf{b}_{lmmse} = \mathbf{A}^T \mathbf{L} E\{\mathbf{r}\} - \mathbf{B}_{lmmse} E\{\mathbf{d}\}, \quad (7)$$

where

$$\mathbf{K}_r = E\{\mathbf{r}\mathbf{r}^T\} - E\{\mathbf{r}\} E\{\mathbf{r}\}^T \quad (8)$$

is the covariance matrix of the radiant spectra as seen by the camera, and

$$\mathbf{K}_n = E\{\mathbf{nn}^T\} \quad (9)$$

is the noise covariance matrix, assuming the noise is zero mean.

Note that if we are working with the recorded value of \mathbf{c}_i from Equation 1, instead of the value of \mathbf{d}_i from Equation 2, then simply replace the matrix \mathbf{M} with matrix \mathbf{H} in the above equations.

In some cases, the spectral sensitivity of the system is not known or is difficult to obtain. In these situations, a linear transformation can be obtained through the use of a data fit on a known set of reflectance spectra. This approach is sometimes referred to as a pseudo-inverse solution [11]. The problem can mathematically be posed as the following: Given a set of measurements \mathbf{d}_i (Equation 2) and \mathbf{t}_i (Equation 3) on samples $i = 1, \dots, p$, the matrix \mathbf{B}_{pseudo} and vector \mathbf{b}_{pseudo} are the solution to the optimization problem

$$(\mathbf{B}_{pseudo}, \mathbf{b}_{pseudo}) = \arg \min_{\mathbf{B}, \mathbf{b}} \sum_{i=1}^p \|\mathbf{B}\mathbf{d}_i + \mathbf{b} - \mathbf{t}_i\|^2. \quad (10)$$

The solution is given by

$$\mathbf{B}_{pseudo} = \mathbf{T} \mathbf{D}^T (\mathbf{D} \mathbf{D}^T)^{-1} \quad (11)$$

$$\mathbf{b}_{pseudo} = \hat{\mathbf{t}}_{avg} - \mathbf{B}_{pseudo} \hat{\mathbf{d}}_{avg}, \quad (12)$$

where

$$\hat{\mathbf{t}}_{avg} = \frac{1}{p} \sum_{i=1}^p \mathbf{t}_i \quad (13)$$

$$\hat{\mathbf{d}}_{avg} = \frac{1}{p} \sum_{i=1}^p \mathbf{d}_i \quad (14)$$

$$\mathbf{T} = [\mathbf{t}_1, \dots, \mathbf{t}_p] - [\hat{\mathbf{t}}_{avg}, \dots, \hat{\mathbf{t}}_{avg}] \quad (15)$$

and

$$\mathbf{D} = [\mathbf{d}_1, \dots, \mathbf{d}_p] - [\hat{\mathbf{d}}_{avg}, \dots, \hat{\mathbf{d}}_{avg}]. \quad (16)$$

A similar fit can be made between the \mathbf{c}_i values (Equation 1) and the \mathbf{t}_i values.

Camera noise model

As previously mentioned, the noise process in a digital camera is signal dependent [1]. The measurement of light on a sensor is an example of a process that counts the number of arrival events. In this case, the accumulated charge for a sensor element is related to the number of photons that arrived at the sensor (and resulted in a charge increase). For a constant light source on a sensor over a fixed period of time, there is a statistical variability in the number of photons that will arrive over that period. This uncertainty can be modeled by a Poisson probability density function (PDF). A Poisson PDF has the property that the mean is equal to the variance. This implies that the variance of the light measurement will depend upon the average level of light on the sensor. At the large counts that are received at the sensor, the Poisson PDF is well approximated by a Gaussian PDF with the variance being a scaled factor of the mean.

For a given camera, one can estimate the relationship between the mean measurement value and the variation of the measurement through the measurement of samples of uniform reflectance. Figure 2 shows such measurements for one channel of a Nikon D750. This plot has the signal mean on the x-axis and the signal variance on the y-axis. The slope of this data is fit with a line, which provides an estimate for the relationship of the signal value to the noise variance for the sensor data.

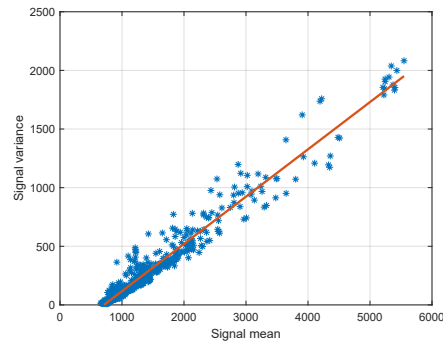


Figure 2. Signal mean vs. signal variance for Nikon D750. Slope of fitted line is 0.4

If the slope of channel k is given by the term α_k , and the noise free measurement is given by the value d_k , then the noise on that sample is modeled with a zero mean Gaussian distribution with a variance given by

$$\sigma_k^2 = \alpha_k d_k. \quad (17)$$

Quantifying system colorimetry

There are several approaches to quantifying the colorimetric accuracy of a camera system. One approach is to make use of the Vora Value, which provides a measure of how well the space defined by the spectral sensitivity of the system matches the space defined by the CIE color matching functions [3]. For a system given by Equation 2, the Vora Value between it and the CIE color matching functions with illuminant \mathbf{L} is

$$v(\mathbf{L}\mathbf{A}, \mathbf{G}) = \frac{\text{Trace} [\mathbf{P}_{\mathbf{L}\mathbf{A}} \mathbf{G} (\mathbf{G}^T \mathbf{G})^{-1} \mathbf{G}^T]}{3}, \quad (18)$$

where $\mathbf{G} = \mathbf{L} [\mathbf{H} \mathbf{H}\mathbf{F}]^T$ and

$$\mathbf{P}_{\mathbf{L}\mathbf{A}} = \mathbf{L}\mathbf{A}(\mathbf{A}^T \mathbf{L}\mathbf{L}\mathbf{A})^{-1} \mathbf{A}^T \mathbf{L}. \quad (19)$$

The term $\mathbf{P}_{\mathbf{L}\mathbf{A}}$ is the orthogonal projection operator onto the subspace defined by the matrix $\mathbf{L}\mathbf{A}$, which is the illuminant multiplied by the CIEXYZ color matching functions. Similarly, the term $\mathbf{G}(\mathbf{G}^T \mathbf{G})^{-1} \mathbf{G}^T$ is the orthogonal projection operator on the subspace defined by the matrix \mathbf{G} . The Vora Value is bounded between zero and one. A value of one indicates that the subspace defined by matrix \mathbf{G} contains the subspace defined by $\mathbf{L}\mathbf{A}$. A value of zero indicates that the subspaces are orthogonal.

Sharma provided a number of Figures of Merit (FOM) that are similar to the Vora Value but take into account the statistics of the spectral data that is being measured as well as the noise statistics [12]. One form of the FOM is given by

$$q(\mathbf{L}\mathbf{A}, \mathbf{G}, \mathbf{K}_r, \mathbf{K}_n) = \frac{\tau(\mathbf{L}\mathbf{A}, \mathbf{G}, \mathbf{K}_r, \mathbf{K}_n)}{\text{Trace} [\mathbf{P}_{\mathbf{L}\mathbf{A}} \mathbf{K}_r]}, \quad (20)$$

where

$$\tau(\mathbf{L}\mathbf{A}, \mathbf{G}, \mathbf{K}_r, \mathbf{K}_n) = \text{Trace} \left[\mathbf{P}_{\mathbf{L}\mathbf{A}} \mathbf{K}_r \mathbf{G} \left(\mathbf{G}^T \mathbf{K}_r \mathbf{G} + \mathbf{K}_n \right)^{-1} \mathbf{G}^T \mathbf{K}_r \right]. \quad (21)$$

Like the Vora Value, this FOM has a maximum of one, indicating an optimal system, and a minimum of zero, indicating a system that would perform poorly.

Another way to quantify the performance of a system is simply to look at the simulated performance of the system on a set of reflectance spectra and compute the color errors that occur. For example, one could use a set of spectra, such as those defined in [13]. If these spectra are defined to be \mathbf{r}_i for $\{i = 1, \dots, p\}$, and the LMMSE estimator is used to map from camera values to CIEXYZ values, then one could use the average ΔE value across the data set as a measure of goodness, which is given by

$$\Delta E_{avg} = \frac{1}{p} \sum_{i=1}^p \|\mathcal{F}(\mathbf{B}_{lmmse} \mathbf{d}_i + \mathbf{b}_{lmmse}) - \mathcal{F}(\mathbf{t}_i)\|, \quad (22)$$

where $\mathcal{F}(\cdot)$ is the vector valued function that maps CIEXYZ values to CIELAB values.

Alternatively, one could use the maximum ΔE value across the data set, which is given by

$$\Delta E_{max} = \max_i \|\mathcal{F}(\mathbf{B}_{lmmse} \mathbf{d}_i + \mathbf{b}_{lmmse}) - \mathcal{F}(\mathbf{t}_i)\|. \quad (23)$$

For accurate modeling, the effects of noise should be included in determining the optimal filter. Noise can be considered by running multiple realizations at a particular signal-to-noise ratio and looking at the resulting statistics.

For example, signal dependent noise could be added to the measurements to provide \mathbf{d}_i values, via Equation 2, for a set of p spectra. Equation 22 is then used to compute the ΔE_{avg} for the set of p spectra. This process is repeated q times, each with a new noise realization, giving q ΔE_{avg} values. The best filter is the filter that minimizes

$$\frac{1}{q} \sum_{i=1}^q \Delta E_{avg}. \quad (24)$$

A similar process can be used for finding the filter that minimizes the maximum error in the presence of noise.

Filters

To focus on filters that can be readily obtained, a software tool provided by the filter manufacturer Hoya Corporation was used to generate filter transmittances. The application allowed the selection of 108 filter types and the specification of the filter thickness. For each filter type, ten filters were computed for thicknesses on a logarithmic scale from a minimum of 0.5 mm to a maximum of 9 mm. (This was the maximum range allowed by the software.)

Given this data set of filters and the spectral response for a Nikon D90, as shown in Figure 3, an exhaustive search was performed to determine the optimal filters using the following specifications:

- Find the filter that provides the largest Vora Value for the camera system. Denote this filter as \mathbf{f}_{VV} .
- Find the filter that provides the largest Figure of Merit for the camera system for a noise slope α . Denote this filter as $\mathbf{f}_{FOM|\alpha}$.
- Find the filter that when used on a large set of reflectance spectra results in the minimum average ΔE_{2000} value on that data set for noise slope α . Denote this filter as $\mathbf{f}_{avg\Delta E00|\alpha}$.
- Find the filter that when used on a large set of reflectance spectra results in the minimum maximum ΔE_{2000} value on that data set with noise slope α . Denote this filter as $\mathbf{f}_{max\Delta E00|\alpha}$.

For our study, we used values for α of [0.0, 0.1, 0.2, 0.3, 0.4] that linearly step from no noise to a noise level typically seen in modern digital cameras [1].

The data set used for the reflectance spectra was from [13], and a uniform illumination was used (meaning an illumination that is spectrally flat). For each noise level, 1000 realizations were run for each filter allowing us to compute average performance across the data set. This data set was defined as the training data

set, since it was used for the filter selection as well as the determination of the LMMSE estimator in the next section. For testing the performance, the reflectance spectra from a Digieye DT (240 color patches) chart were used to assess the robustness of the solution.

The Vora filter and FOM filters are shown in Figure 4. The best Vora Value filter was a green filter with a peak wavelength around 535 nm. In the presence of noise, the FOM filters tended to pass all wavelengths with a possible reduction in the red wavelengths. The filters that do best in terms of ΔE_{2000} were yellow in nature and are shown in Figure 5. With noise present in the system, the 50% cutoff of these filters ranged from 460 nm to 480 nm.

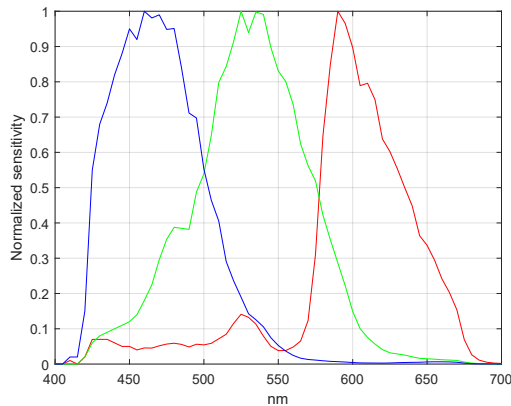


Figure 3. Nikon D90 camera spectral sensitivities

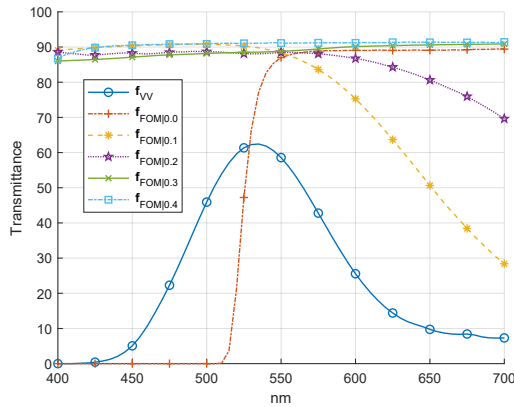


Figure 4. Selected filters using Vora Value and FOM

For a given filter, the spectral response of the system is the combination of the camera with and without the filter. For each system response, the orthogonal projection onto the space defined by the CIEXYZ color matching functions of the six-band system was performed. The projections for three representative cases are shown in Figures 6—8. For comparison, the orthogonal projection of the unfiltered camera system is shown in Figure 9. These plots represent a visual display of how well the spectral response

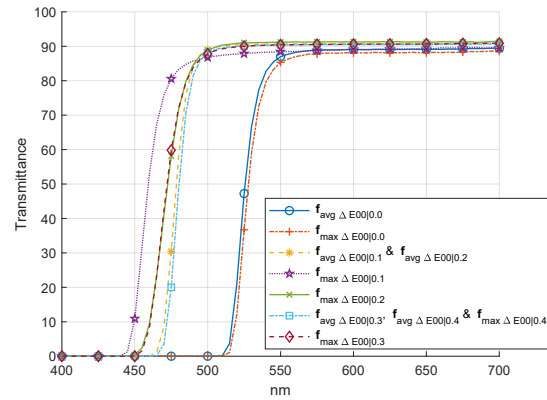


Figure 5. Selected filters using ΔE statistics

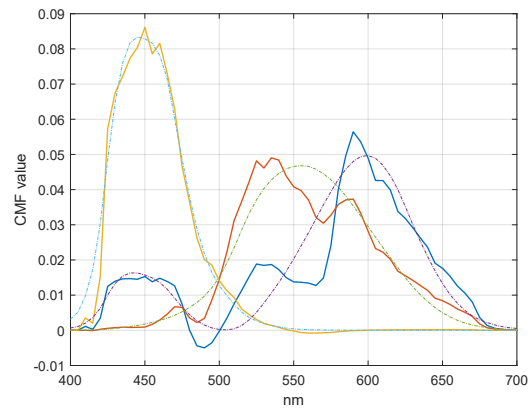


Figure 6. Projection of Nikon D90 camera spectral sensitivities with and without $f_{avg \Delta E(0.4)}$ filter onto space defined by CIEXYZ color matching functions

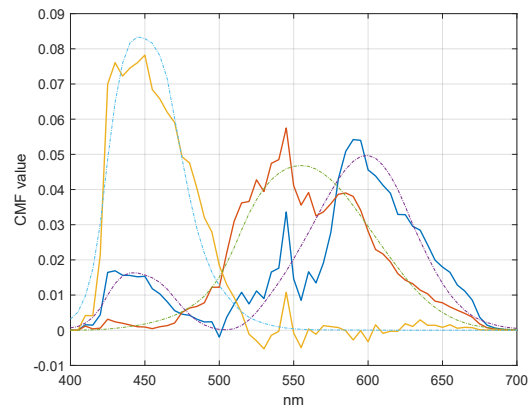


Figure 7. Projection of Nikon D90 camera spectral sensitivities with and without $f_{FOM(0.4)}$ filter onto space defined by CIEXYZ color matching functions

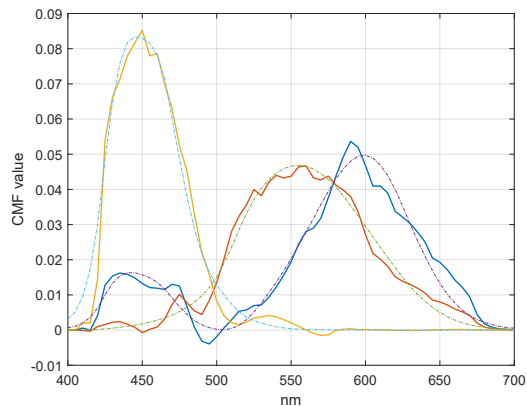


Figure 8. Projection of Nikon D90 camera spectral sensitivities with and without f_{VV} filter onto space defined by CIEXYZ color matching functions

of the system can approximate the CIEXYZ color matching functions in a least-squares sense. Subjectively, using the Vora Value filter provides the best looking approximation to the CIEXYZ color matching functions (Figure 8).

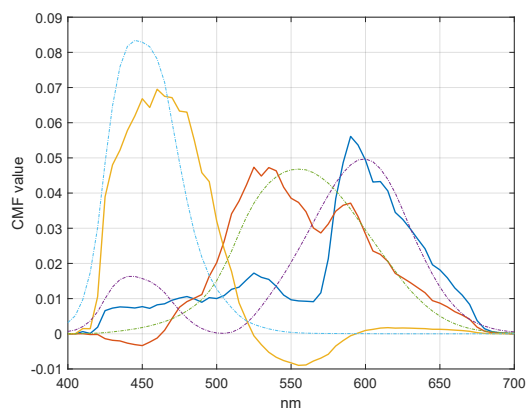


Figure 9. Projection of Nikon D90 camera spectral sensitivities onto space defined by CIEXYZ color matching functions

Simulations

The filters found above were used in a simulation process, whereby reflectance spectra were mathematically recorded at noise levels of α equal to [0.0, 0.1, 0.2, 0.3, 0.4]. Recordings were done with and without the filter, which provided six bands of information for each case. The illumination used for recording and as a target to map to was the uniform illuminant (meaning an illumination that is spectrally flat). As mentioned in the previous section, a Digieye DT (240 color patches) chart was used for testing the performance and the set from [13] was used as a training data set to determine the LMMSE estimator.

The LMMSE estimator was used to transform the simulated recorded values of the testing and training data to CIEXYZ values. CIE ΔE_{2000} values were computed across the testing and training

data sets. From these values, an average and max ΔE_{2000} value was computed. To quantify the performance of the system under noise, this simulation process was repeated 1000 times and the average and max ΔE_{2000} values were averaged across the noise realizations. The results for the training data are given in Table 1, and the results for the testing data are given in Table 2. The smallest errors within each noise level section are shown in bold red entries. The last column in the table shows the percent reduction in the average ΔE_{2000} error compared to the no-filter case.

With no noise, the improvement from capturing another image with the filter is significant. This is true for the training and the testing data, regardless of the approach used to select the filter. When noise is introduced, the performance of all the filters is significantly reduced, but still provide improvement. On the testing data, the FOM filter performs significantly worse compared to the other filters. The Vora Value filter, which does not consider the data set nor the noise level, does well at all noise levels and for the training and testing data set. The filters that minimized the average ΔE_{2000} error on the noisy training data did the best on the testing data. In the testing and training data sets, these filters were always equal to or better than the theoretical criteria (Vora and FOM filters).

It should be noted that when noise is present in the system, one could capture two no-filter images and average these two images to reduce the noise level. The effect would be equivalent to reducing the α value by a factor of two. Meaning that taking two no-filter images at an α value of 0.4 and creating one image would provide the same performance as an α value of 0.2 (likewise, two images at α of 0.2 would provide the same performance as α of 0.1). Note that this performance reduction is in regard to the mean squared error in CIEXYZ space not necessarily ΔE . From the results in the table, the Vora Value filter and the filters that minimize ΔE_{2000} error still perform better on the testing data set compared to the lower noise, no-filter case (meaning we are better off using an appropriately shaped filter rather than capturing two no-filter images). Likewise, since the FOM filter at higher noise levels is almost spectrally flat, its performance is similar to the no-filter case at a noise level that is half the FOM filter noise level — and the FOM filter does not do as well as the Vora Value or minimum ΔE filters, at the higher noise levels.

Summary

The results of these simulations indicate that the use of an additional external filter when capturing an image with a digital camera can provide data that allows for improved colorimetry even in the presence of noise. With no noise present in the system, the average ΔE_{2000} errors on the testing data were reduced by 86%. With noise levels found in a typical imaging system, the average ΔE_{2000} errors on the testing data were reduced by 38%. The FOM filter did not perform as well as the Vora Value filter in the presence of noise, which was unexpected, since the FOM filter is selected using knowledge about the level of noise in the system. This result warrants further research. The next step in this work is to capture image data with and without an optimally determined filter and to apply the necessary processing steps on that image data to provide an image with improved colorimetry.

Table 1: Simulation results training data [smallest errors given in red]

Filter	α	Avg. ΔE_{2000}	Max. ΔE_{2000}	Avg. ΔE_{2000} % Reduction
No-filter	0.0	0.69	7.65	0%
f_{VV}	0.0	0.17	3.00	75.4%
$f_{FOM 0.0}$	0.0	0.11	1.06	84.1%
$f_{avg\Delta E00 0.0}$	0.0	0.11	1.06	84.1%
$f_{max\Delta E00 0.0}$	0.0	0.11	1.06	84.1%
No-filter	0.1	1.08	7.91	0%
f_{VV}	0.1	0.81	4.10	25.0%
$f_{FOM 0.1}$	0.1	0.92	9.54	14.8%
$f_{avg\Delta E00 0.1}$	0.1	0.73	4.62	32.4%
$f_{max\Delta E00 0.1}$	0.1	0.75	3.92	30.6%
No-filter	0.2	1.32	8.10	0%
f_{VV}	0.2	1.08	5.42	18.2%
$f_{FOM 0.2}$	0.2	1.10	7.80	16.7%
$f_{avg\Delta E00 0.2}$	0.2	0.96	5.14	27.3%
$f_{max\Delta E00 0.2}$	0.2	0.97	5.02	26.5%
No-filter	0.3	1.52	8.32	0%
f_{VV}	0.3	1.28	6.36	15.8%
$f_{FOM 0.3}$	0.3	1.23	8.11	19.1%
$f_{avg\Delta E00 0.3}$	0.3	1.14	5.89	25.0%
$f_{max\Delta E00 0.3}$	0.3	1.15	5.89	24.3%
No-filter	0.4	1.69	8.63	0%
f_{VV}	0.4	1.44	7.12	14.8%
$f_{FOM 0.4}$	0.4	1.34	8.14	20.7%
$f_{avg\Delta E00 0.4}$	0.4	1.29	6.55	23.7%
$f_{max\Delta E00 0.4}$	0.4	1.29	6.55	23.7%

Table 2: Simulation results testing data [smallest errors given in red]

Filter	α	Avg. ΔE_{2000}	Max. ΔE_{2000}	Avg. ΔE_{2000} % Reduction
No-filter	0.0	1.09	5.54	0%
f_{VV}	0.0	0.18	0.69	83.5%
$f_{FOM 0.0}$	0.0	0.15	0.53	86.2%
$f_{avg\Delta E00 0.0}$	0.0	0.15	0.53	86.2%
$f_{max\Delta E00 0.0}$	0.0	0.15	0.54	86.2%
No-filter	0.1	1.36	5.66	0%
f_{VV}	0.1	0.71	2.64	47.8%
$f_{FOM 0.1}$	0.1	1.11	4.76	18.4%
$f_{avg\Delta E00 0.1}$	0.1	0.64	2.50	52.9%
$f_{max\Delta E00 0.1}$	0.1	0.69	2.50	49.3%
No-filter	0.2	1.54	5.84	0%
f_{VV}	0.2	0.95	3.54	38.3%
$f_{FOM 0.2}$	0.2	1.36	5.59	11.7%
$f_{avg\Delta E00 0.2}$	0.2	0.83	3.15	46.1%
$f_{max\Delta E00 0.2}$	0.2	0.84	3.21	45.5%
No-filter	0.3	1.68	6.06	0%
f_{VV}	0.3	1.14	4.19	32.1%
$f_{FOM 0.3}$	0.3	1.48	5.83	11.9%
$f_{avg\Delta E00 0.3}$	0.3	0.99	3.73	41.1%
$f_{max\Delta E00 0.3}$	0.3	1.00	3.83	40.5%
No-filter	0.4	1.81	6.32	0%
f_{VV}	0.4	1.29	4.72	28.7%
$f_{FOM 0.4}$	0.4	1.56	5.88	13.8%
$f_{avg\Delta E00 0.4}$	0.4	1.12	4.23	38.1%
$f_{max\Delta E00 0.4}$	0.4	1.12	4.23	38.1%

References

- [1] H. J. Trussell and R. Zhang, "The dominance of Poisson noise in color digital cameras," 2012 IEEE Int. Conf. Image Process., pp. 329-332, (2012).
- [2] R. Luther, "Aus dem Gebiet der Farbreizmetrik," Zeitschrift für Technische Physik, vol. 8, pp. 540-558, (1927).
- [3] P. L. Vora and H. J. Trussell, "Measure of goodness of a set of color scanning filters," J. Opt. Soc. Amer. A, vol. 10, no. 7, pp. 1499-1508, (1993).
- [4] G. D. Finlayson, Y. Zhu, and H. Gong, "Using a simple colour pre-filter to make cameras more colorimetric," IS&T 26th Color and Imaging Conference, pp. 182-186, (2018).
- [5] G. D. Finlayson and Y. Zhu, "Finding a colour filter to make a camera colorimetric by optimisation," International Workshop on Computational Color Imaging., Springer, pp. 53-62, (2019).
- [6] G. D. Finlayson and Y. Zhu, "Designing color filters that make cameras more colorimetric," IEEE Trans. Image Process., vol. 30, pp. 853-867, (2021).
- [7] Y. Zhu and G. Finlayson, "An improved optimization method for finding a color filter to make a camera more colorimetric," Electronic Imaging 2020, pp. (163)1-6, (2020).
- [8] M. J. Vrhel, "Improved camera color accuracy in the presence of noise with a color prefilter," IS&T 28th Color and Imaging Conference, pp. 187-192, (2020).

- [9] M. J. Vrhel, H. J. Trussell, and J. Bosch, "Design and realization of optimal color filters for multi-illuminant color correction," J. Electron. Imag., vol. 4, pp. 6-14, Jan. (1995).
- [10] H. J. Trussell and M. S. Kulkarni, "Sampling and processing of color signals," IEEE Trans. Image Process., vol. 5, no. 4, pp. 677-681, April (1996).
- [11] H. J. Trussell and R. Shamey, "Accurate colorimetric images using LEDs," Journal of Electronic Imaging, vol. 29, no. 4, pp. (043008)1-16, July (2020).
- [12] G. Sharma and H. J. Trussell, "Figures of merit for color scanners," IEEE Trans. Image Process., vol. 6, no. 7, pp. 990-1001, July (1997).
- [13] D. Wüller, "In situ measured spectral radiation of natural objects," IS&T 17th Color and Imaging Conference, pp. 159-163, November (2009).

Author Biography

Michael Vrhel was awarded his PhD from North Carolina State University in 1993; during his PhD, he was an Eastman Kodak Fellow. He has many years' experience working in digital imaging, including biomedical imaging and signal processing at NIH; color instrument and color software design at Color Savvy Systems Ltd, and positions at Conexant Systems, TAK Imaging and Artifex Software. A senior member of the IEEE, he has a number of current and pending patents and is the author of numerous papers in the areas of image and signal processing including a book,

The Fundamentals of Digital Imaging. His current interests include efficient computational color rendering methods as well as deep learning applications.

H. Joel Trussell received his PhD in electrical engineering and computer science from the University of New Mexico, Albuquerque, New Mexico, USA, in 1976. Currently, he is an emeritus professor in electrical and computer engineering, NC State University. He has a long research history in signal and image processing and a shorter history in education, publishing over 200 papers in refereed journals and conferences. He is a fellow of the IEEE.